Distributions of polymers in disordered structures

H. Eduardo Roman,[1] Julia Dräger,[1,2] Armin Bunde,[1] Shlomo Havlin,[1,3] and Dietrich Stauffer[4]
[1]*Institut für Theoretische Physik, Justus-Liebig-Universität Giessen, D-35392 Giessen, Germany*
[2]*I. Institut für Theoretische Physik, Universität Hamburg, D-20355 Hamburg, Germany*
[3]*Department of Physics, Bar-Ilan University, Ramat Gan, Israel*
[4]*Institut für Theoretische Physik, Universität Köln, D-50923 Köln, Germany*
(Received 19 May 1995)

We study the behavior of linear polymers (modeled by self-avoiding random walks of N steps) on random fractal structures, both in Euclidean metric (r space) and "chemical" metric (l space). The chemical distance l between two sites on the structure at distance r from each other is the length of the shortest path connecting them, $l \sim r^{d_{\min}}$, where $d_{\min}$ is the fractal dimension of the shortest path. We consider the average probabilities $\langle P(l,N)\rangle$ and $\langle P(r,N)\rangle$ to find a polymer of N monomers having a chemical end-to-end distance l or an Euclidean end-to-end distance r, respectively. We also study the first moments $\langle l(N)\rangle$ and $\langle r(N)\rangle$ of these probabilities. Our numerical results, obtained for two-dimensional percolation clusters at criticality, show that the fluctuations in l space are considerably smaller than in r space, suggesting that the l metric is more appropriate for studying structural properties of polymers in disordered media. We find $\langle l(N)\rangle \sim N^{\nu_l}$, with $\nu_l = 0.87 \pm 0.02$, and $\langle P(l,N)\rangle \sim (1/l) y^{g_l}$ when $y < 0.35$, and $\langle P(l,N)\rangle \sim (1/l) y^{g_l'} \exp(-b y^{\delta_l})$ when $y > 0.35$, where $y \equiv l/N^{\nu_l}$, $g_l = 2.5 \pm 0.2$, $g_l' = 3.0 \pm 0.2$, and $\delta_l = 1/(1-\nu_l)$. From this form, we show analytically that $\langle P(r,N)\rangle \sim (1/r) x^{g_r} \exp(-c x^{\delta_r})$, where $x \equiv r/N^{\nu_r}$, $\nu_r = \nu_l/d_{\min}$, $g_r = g_l d_{\min}$, and $\delta_r = 1/(1-\nu_r)$. Here $d_{\min} \cong 1.13$. These predictions are supported by the numerical simulations in r space, which yield $\nu_r = 0.76 \pm 0.02$ and $g_r = 2.9 \pm 0.2$. We also derive analytically the way the number of configurations taken in the averages affects the exponent δ_r.

PACS number(s): 05.40.+j, 05.50.+q, 05.60.+w

I. INTRODUCTION

In past years, the question how linear polymers behave in disordered media that are self-similar on certain length scales has attracted much attention (for recent reviews see [1,2] and references cited therein). So far, most of the work has been concentrated on the problem how the mean end-to-end distance of the chain $\langle r(N)\rangle$ depends on the number of monomers N of the polymer.

From a microscopic point of view, more important is the configurational averaged distribution function $\langle P(r,N)\rangle$, which is defined as the probability that a polymer of N monomers has an end-to-end distance r. The mean end-to-end distance $\langle r(N)\rangle$ is only the first moment of $\langle P(r,N)\rangle$ and contains only part of the information. While the distribution function has been well studied in regular ordered systems [3–13], not much is known about the functional form of $\langle P(r,N)\rangle$ in disordered systems [1,2].

In contrast, the analogous problem of the distribution function of random walks *without* the self-avoiding constraint has been studied extensively, also in disordered systems that are fractal on certain length scales [14–20]. It has been found that in order to understand the complex behavior of $\langle P(r,N)\rangle$ it is crucial to know the behavior in *chemical* l space [16,17,20], which is simpler and easier to obtain. The chemical distance l between two sites on a structure separated by the (Euclidean) distance r is defined as the length of the shortest path on the structure connecting them. The average $\langle l(r)\rangle$ scales as $\langle l(r)\rangle \sim r^{d_{\min}}$ where $d_{\min}$ is the fractal dimension of the shortest path [14]. It has been shown for random walks on random fractals that the probability $P_i(l,N)$ to find a random walker after N time steps on a site i at chemical distance l varies little within one configuration and between different configurations [16]. Using this fact, one can deduce, via convolutional integrals, analytical expressions for the relevant probability distribution $\langle P(r,N)\rangle$.

Here we show that the shortest path metric (l space) is also useful to study polymers modeled by self-avoiding random walks (SAWs) in disordered structures. We introduce the quantity $\langle P(l,N)\rangle$, which is defined as the probability that the two ends of a polymer of N monomers are separated by the chemical distance l, averaged over many configurations of the substrate. We find that, similar to the random walk case, the fluctuations in l space are significantly smaller than the fluctuations in r space and derive an analytical expression for the asymptotic behavior of $\langle P(r,N)\rangle$.

The paper is organized as follows. To test our method of generating SAWs we first study (Sec. II) SAWs on the regular square lattice. Next, in Sec. III, we present analytical and numerical results for SAWs in two-dimensional (2D) percolation, both in l and r space, and show how the mean distribution functions in l and r space are related. Finally, in Sec. IV, we present some concluding remarks.

II. SAWS ON REGULAR LATTICES

Polymers consisting of N monomers are commonly modeled by N-step SAW. The set of N-step SAWs is

defined as the subset of all random walks of N steps that do not self-intersect. However, to generate long SAWs by generating all random walks, is numerically unpractical since the probability to obtain such SAWs decreases exponentially with N. We therefore generated SAWs by the enrichment method [21]. First, n-step random walks are generated until a random walk without self-intersections is obtained. Next, from the end point of this self-avoiding random walk, another n-step random walk is started. If this second n-step walk does not intersect with itself and with the first n-step walk, we have obtained a $2n$-step SAW this way. Otherwise, we try again, but only k trials are allowed. If the procedure fails, we start from the very beginning. This process continues to obtain $3n$-, $4n$-,... step SAWs until the desired SAW of N steps is achieved.

To test our approach, we first studied the mean end-to-end distance $\langle r(N)\rangle$ and the probability distribution $P(r,N)$ on a square lattice ($d=2$), where $r\sim l$ and analytical results are available. Figure 1(a) shows $\langle r(N)\rangle$ as a function of N. The asymptotic straight line on the double-logarithmic plot represents the known scaling proportionality

$$\langle r\rangle \sim N^{\nu} , \tag{1}$$

with $\nu=\frac{3}{4}$, which is in excellent agreement with our numerical simulation. Figure 1(b) shows the probability distribution $P(r,N)$. As seen in the figure, the simulations support the overall scaling approximation

$$P(r,N)=(A/r)(r/N^{\nu})^{g}\exp[-a(r/N^{\nu})^{\delta}] , \tag{2}$$

with $\nu=0.75$, $\delta=1/(1-\nu)=4$, and $g=d+\vartheta$, where $\vartheta=0.6\pm0.1$, in agreement with the theoretical predictions [3–6]. The prefactor $\sim 1/r$ is required to ensure the normalization $\int dr\, P(r,N)=1$. The overall agreement between the data and the theory strongly supports the accuracy of the enrichment method. We notice that for $r/N^{\nu}\ll 1$ the exponent ϑ is expected to be smaller $\vartheta\cong\frac{4}{9}$ [5,6]. However, because of the relatively short SAW chains that we have used we cannot determine such a value accurately. For further numerical results related to this problem see, e.g., Ref. [8].

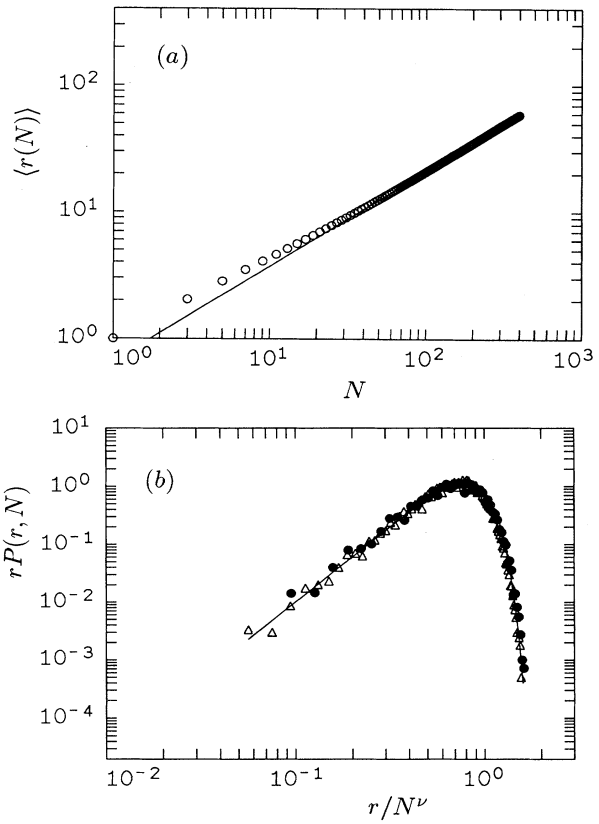

FIG. 1. (a) Plot of $\langle r(N)\rangle$ versus N on a double-logarithmic graph. The circles represent data from simulations of SAWs on a regular square lattice. The line represents the theoretical prediction with slope $\nu=0.75$. The averages include 10^6 SAW configurations of 400 steps. The walks were generated with the enrichment parameters $k=1000$ and $n=40$. (b) Plot of $rP(r,N)$ versus r/N^{ν} on a double-logarithmic graph. The circles represent the numerical data for $N=100$ and the triangles for $N=200$. The line represents the analytical expression Eq. (2) with $\nu=0.75$, $\delta=4$, $g=2.6\pm0.1$, $A=4.0\pm0.5$, and $a=1.60\pm0.3$.

III. SAWS IN 2D PERCOLATION CLUSTERS AT CRITICALITY

Next we used the enrichment method to study SAWs in disordered media, modeled by the incipient percolation cluster on a square lattice (see, e.g. [17]). Figure 2(a) shows that the mean chemical end-to-end distance $\langle l(N)\rangle$ follows a power law

$$\langle l(N)\rangle \sim N^{\nu_l} , \tag{3a}$$

with $\nu_l=0.87\pm0.02$, in agreement with theoretical predictions based on Flory-type arguments [14]

$$\nu_l=\frac{2+v/d_w^{lB}}{v+d_l^{B}} , \tag{3b}$$

where $v=d_w^{lB}/(d_w^{lB}-1)$ and d_l^{B} and d_w^{lB} are the chemical dimension and the anomalous diffusion exponent of the percolation backbone. The backbone exponents control the SAW exponents on percolation since an infinite SAW can exist only on the percolation backbone [14]. Equation (3b) predicts the following values for ν_l. In $d=2$, we have $d_l^{B}\cong 1.42$ and $d_w^{lB}\cong 2.37$, yielding $\nu_l\cong 0.87$. In $d=3$, we have $d_l^{B}\cong 1.29$ and $d_w^{lB}\cong 2.27$, yielding $\nu_l\cong 0.90$. Note that for $d\geq 6$, we have $d_l^{B}=1$ and $d_w^{lB}=2$, yielding $\nu_l=1$.

Since $l\sim r^{d_{\min}}$, we expect

$$\langle r(N)\rangle \sim N^{\nu_r} , \tag{4a}$$

where

$$\nu_r=\nu_l/d_{\min} . \tag{4b}$$

For $d=2$, $d_{\min}=1.133\pm0.002$ [22], which yields $\nu_r=0.77\pm0.02$. This result is consistent with other values reported recently in the literature (see [1,2] and

references therein). For $d=3$, $d_{\min}=1.35\pm0.03$ [22], which yields $\nu_r=0.67\pm0.03$. For $d\geq 6$, $d_{\min}=2$ and thus $\nu_r=\frac{1}{2}$.

Next we discuss the average probability $\langle P(l,N)\rangle$ that the end point of a SAW of N steps is at a chemical distance l from its starting point. To obtain $\langle P(l,N)\rangle$, we averaged over 1000 realizations of SAWs on 1000 percolation clusters each. Figure 2(b) shows $l\langle P(l,N)\rangle$ versus l/N^{ν_l} and suggests that for $l/N^{\nu_l}>0.35$,

$$\langle P(l,N)\rangle \simeq (B'/l)(l/N^{\nu_l})^{g_l'}\exp[-b(l/N^{\nu_L})^{\delta_l}] , \quad (5a)$$

with $\delta_l=1/(1-\nu_l)$, $B'=1.6\pm0.5$, $g_l'=3.0\pm0.2$, and $b=0.16\pm0.03$. For $l/N^{\nu_l}<0.35$, the data suggest that

$$\langle P(l,N)\rangle \simeq (B/l)(l/N^{\nu_l})^{g_l} , \quad (5b)$$

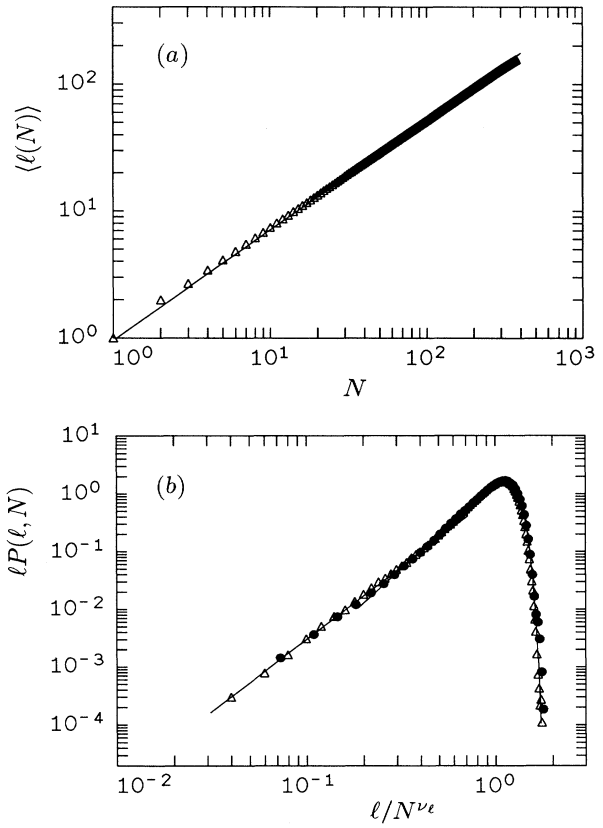

FIG. 2. (a) Plot of $\langle l(N)\rangle$ versus N on a double-logarithmic graph for SAWs on two-dimensional percolation clusters at criticality, grown on a square lattice up to 400 chemical shells. The triangles are the numerical data while the line is a best fit with a slope $\nu_l=0.87\pm0.02$. The chains were generated with enrichment parameters $k=1000$ and $n=5$ up to a maximum number of $N=400$ SAW steps. (b) Plot of $l\langle P(l,N)\rangle$ versus l/N^{ν_l} on a double-logarithmic graph. The circles represent the numerical data for $N=100$ and the triangles for $N=200$. The dashed line represents the functional form $B'x^{g_l'}\exp(-bx^{\delta_l})$ [Eq. (5a)], where $x=l/N^{\nu_l}$, with $\nu_l=0.87\pm0.02$, $\delta_l=1/(1-\nu_l)$, $g_l'=3.0\pm0.2$, $B'=1.6\pm0.5$, and $b=0.16\pm0.03$. For $x<0.35$, a smaller value of the exponent g_l represents the data better and we find $g_l=2.5\pm0.2$ and $B=0.95\pm0.5$ [Eq. (5b)].

with $B=0.95\pm0.5$ and $g_l=2.5\pm0.2$. Notice that $\langle P(l,N)\rangle$ is normalized according to $\int dl\langle P(l,N)\rangle=1$.

In order to learn about the fluctuations in l space, we calculated the number $H(\ln P)d\ln P$ of sites at fixed chemical distance l from the origin, being reached after N SAW steps, with probabilities between $\ln P$ and $\ln P+d\ln P$. Similarly for $P(r,N)$, we calculated the analogous histogram for sites on the same cluster at a fixed Euclidean distance r from the origin. Figure 3 shows the histograms $H(\ln P)$ for SAWs of $N=50$ steps on three typical percolation clusters, with $l=30$ [Fig. 3(a)] and $r=19$ [Fig. 3(b)]. We see that the histogram $H(\ln P)$ is much narrower in l space than in r space. While sites i at fixed chemical distance l from the origin have close probabilities to be reached by the SAW, the probabilities at fixed r fluctuate strongly. A similar behavior was found earlier for random walks on percolation clusters [16].

Next we wish to use the form found for $\langle P(l,N)\rangle$ and the fact that $H(\ln P)$ in l space is relatively narrow to learn about the analogous function in r space, $\langle P(r,N)\rangle$. The approach is similar to that derived in Refs. [16,17,20]; see also Ref. [14]. We define the probability $P_i(r,N)$ that after N steps the SAW has arrived at a backbone site i at distance r from the origin of the SAW, on a given configuration. Assuming that there are N_r^B sites on the backbone at distance r in the considered configuration, the probability $P(r,N)$ for that configuration is simply

$$P(r,N)=\sum_{i=1}^{N_r^B} P_i(r,N) . \quad (6)$$

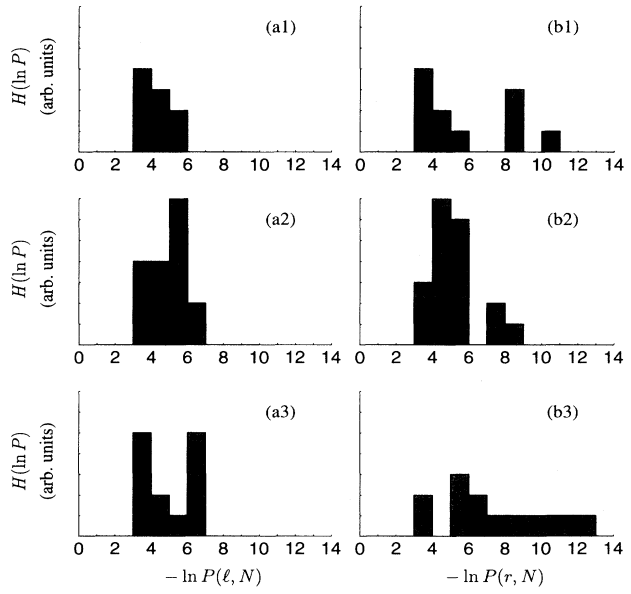

FIG. 3. Histograms of the number of sites having the value (a) $-\ln P(l,N)$ for $N=50$ and $l=30$ and (b) $-\ln P(r,N)$ for $N=50$ and $r=19$. Shown are results of 10^6 SAW configurations on three typical two-dimensional percolation clusters at criticality.

Among the N_r^B sites there are $N_l^B(r)$ sites at chemical distance l from the center and we can write

$$P(r,N)=\sum_{l=l_{\min}(r)}^{\infty} N_l^B(r)P_i(l,N)$$
$$=\sum_{l=l_{\min}(r)}^{\infty}[N_l^B(r)/N_l^B]P(l,N)\ . \quad (7)$$

In deriving the second equality, we have assumed that there are N_l^B sites at chemical distance l from the center and that $P_i(l,N)\simeq P(l,N)/N_l^B$. This is justified since the fluctuations of $P_i(l,N)$ are small. By definition, $l_{\min}(r)$ is the length of the shortest chemical path between the center and any site i on the backbone at fixed distance r in the considered configuration. Assuming further that, similar to the random-walk case, the fluctuations of $P(l,N)$ between different configurations are small, we can write $P(l,N)\simeq\langle P(l,N)\rangle$. Averaging over $N_{\rm av}$ configurations and replacing the sum in (7) by an integral yields the desired relation between $\langle P(l,N)\rangle$ and $\langle P(r,N)\rangle$,

$$\langle P(r,N)\rangle=\int_{l\min}^{\infty}\phi^B(r/l)P(l,N)dl\ , \quad (8)$$

where $\phi^B(r|l)\equiv N_l^B(r)/N_l^B$ is the probability that two sites on the backbone separated by chemical distance l are at Euclidean distance r. The analogous quantity was studied intensively for the structure of the infinite percolation cluster at criticality [14,20,23,24]. We expect a similar functional form for the percolation backbone

$$\phi^B(r|l)=(C_1^B/r)(r/l^{1/d_{\min}})^{g^B}\exp[-C_2^B(r/l^{1/d_{\min}})^{\delta}]\ , \quad (9)$$

with $d=d_{\min}/(d_{\min}-1)$. For fixed r, $\phi^B(r|l)$ has a maximum at $l_{\max}(r)=\alpha_{\max}r^{d_{\min}}$, where $\alpha_{\max}=(\delta C_2^B/g^B)^{d_{\min}-1}$. The lower integration limit in (8), $l_{\min}=l_{\min}(r,N_{\rm av})$, is that of the backbone, which is by definition the same as for the whole percolation cluster. It has been shown in [20] that $l_{\min}$ depends on $N_{\rm av}$ in the following way:

$$l_{\min}(r,N_{\rm av})\simeq\begin{cases}r, & \ll r_c(N_{\rm av})\\ r_c(r/r_c)^{d_{\min}}, & r\gg r_c(N_{\rm av})\ ,\end{cases} \quad (10)$$

where

$$r_c(N_{\rm av})=(\ln z+\ln N_{\rm av})/\ln(1/p_c)\ . \quad (11)$$

Here z is the lattice coordination and p_c is the critical concentration ($p_c\cong 0.593$ for the square lattice).

For evaluating (8), we follow the procedure described earlier in Refs. [14,16,20]. For $l_{\min}(r,N_{\rm av})<l<l_{\max}(r)$, the integrand in (8) is the product of two exponential functions, which shows a steep maximum at $l^*=\xi_r^{d_{\min}}(r/\xi_r)^{\delta_r/\delta_l}$, with $\delta_r=1/(1-\nu_r)$ and $\xi_r=N^{\nu_r}\{C_2^B/[b\delta_l(d_{\min}-1)]\}^{(1-\nu_l)/d_{\min}}\equiv N^{\nu_r}/c^{1/\delta_r}$. Applying the method of steepest descent, we obtain

$$\ln\langle P(r,N)\rangle\simeq -c\left[\frac{r}{N^{\nu_r}}\right]^{\delta_r}\ . \quad (12)$$

By definition, Eq. (12) holds only for l^* between $l_{\min}(r,N_{\rm av})$ and $l_{\max}(r)$ and this condition then determines the r regime $r_0<r<r_\times(N_{\rm av})$, where (12) is valid. We find

$$r_0=\xi_r[g^B/C_s^B\tilde{\delta}]^{1/\delta_r} \quad (13a)$$

and

$$r_\times(N_{\rm av})=\xi_r r_c^{1/\delta_r}(N_{\rm av})\ . \quad (13b)$$

Equation (12) represents only the exponential part of $\langle P(r,N)\rangle$. It is expected that, similar to Eqs. (2) and (5), this exponential will be multiplied by a power-law in the scaling variable r/N^{ν_r}. Thus we expect

$$\langle P(r,N)\rangle=(C/r)(r/N^{\nu_r})^{g_r}\exp[-c(r/N^{\nu_r})^{\delta_r}]\ . \quad (14)$$

In Fig. 4(a) we show results for $\langle r(N)\rangle$ indicating a

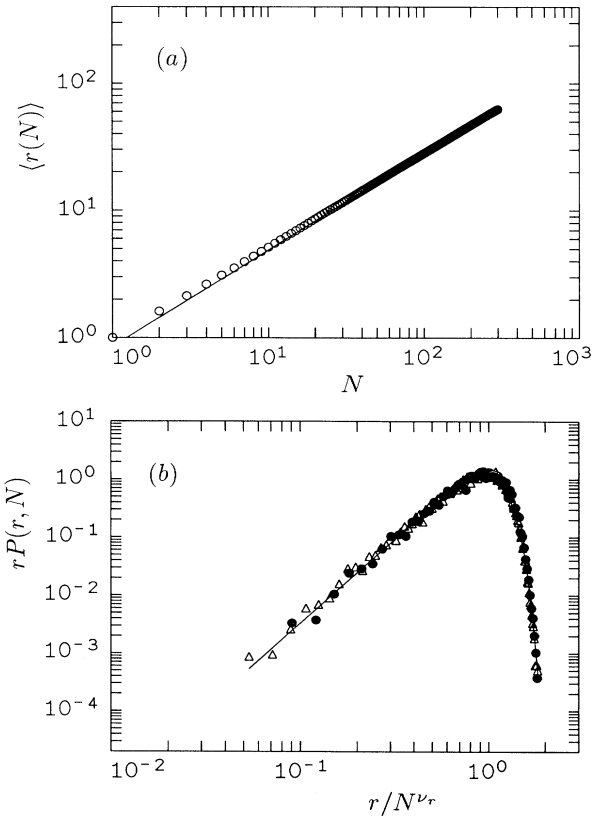

FIG. 4. (a) Plot of $\langle r(N)\rangle$ versus N on a double-logarithmic scale on two-dimensional percolation clusters at criticality. The circles represent the numerical data and the line is a best fit with a slope $\nu_r=0.76\pm0.02$, for the same chains and clusters considered in Fig. 2. (b) Plot of $r\langle P(r,N)\rangle$ versus r/N^{ν_r} on a double logarithmic graph. The circles represent the numerical data for $N=100$ and the triangles for $N=200$. The line represents the analytical function Eq. (14), which fits the data for all r/N^{ν_r}, with $\nu_r=0.76\pm0.02$, $\delta_r=1/(1-\nu_r)$, $g_r=2.9\pm0.2$, $C=2.7\pm0.5$, and $c=0.85\pm0.05$.

power law $\langle r(N)\rangle \sim N^{\nu_r}$ and yielding $\nu_r = 0.76 \pm 0.02$, consistent with our result Eq. (3a) and the prediction (4). Figure 4(b) shows $r\langle P(r,N)\rangle$ versus r/N^{ν_r}. The figure supports our scaling result (14). Moreover, the exponents g_l and g_r describing the small l and r behavior in Eqs. (5b) and (14) can be related to each other from the approximation $\langle P(r=1,N)\rangle = \langle P(l=1,N)\rangle$, yielding

$$g_r = g_l d_{\min} . \tag{15}$$

Our numerical results yield $g_l = 2.5 \pm 0.2$ and $g_r = 2.9 \pm 0.2$, in good agreement with the prediction Eq. (15).

For $r > r_\times(N_{\rm av})$, the integrand in (8) is peaked sharply at $l = l_{\min}(r, N_{\rm av})$ and we predict theoretically

$$\ln\langle P(r,N)\rangle \sim -[l_{\min}(r,N_{\rm av})/N^{\nu_l}]^{\delta_l} \sim -r_c(N_{\rm av})^{\delta_l(1-d_{\min})}(r/\xi_r)^{\delta_l d_{\min}} , \tag{16}$$

where now the exponent in the exponential becomes $\delta_l d_{\min} \cong 8.7$, much larger than $\delta_r \cong 4.3$ in (12). This behavior, however, cannot be seen in the figure since $r_\times(N_{\rm av}) \simeq 2\xi_r$ and we can only reach r values below $r \simeq 2\xi_r$ with the present data.

IV. SUMMARY AND CONCLUSIONS

We have presented analytical and numerical arguments showing that the chemical metric is useful to characterize SAWs in disordered structures. We find that SAWs in l space display fewer fluctuations than in r space and therefore both $\langle l(N)\rangle$ and the probability density $\langle P(l,N)\rangle$ can be studied more accurately. From the form of $\langle P(l,N)\rangle$ we have derived analytical expressions for the average probability density in r space, $\langle P(r,N)\rangle$, which are supported by numerical simulations. The above findings are analogous to those found for random walks in disordered structures.

The analytical forms found here [Eq. (5) and (14)] for $\langle P(r,N)\rangle$ and $\langle P(l,N)\rangle$ for SAWs on percolation have the same functional form as $P(r,N)$ for SAWs on regular lattices, but with different exponents mainly related to the percolation backbone. We have also presented a theory, analogous to that in Ref. [20], for the asymptotic form Eq. (16) of the distribution function $\langle P(r,N)\rangle$ as a function of the number $N_{\rm av}$ of configurations over which averages are performed.

[1] H. Nakanishi, in *Annual Reviews of Computational Physics,* edited by D. Stauffer (World Scientific, Singapore, 1994).
[2] K. Barat and B. K. Chakrabarti (unpublished).
[3] M. E. Fisher, J. Chem. Phys. **44**, 616 (1966).
[4] D. S. McKenzie, Phys. Rep. C **27**, 36 (1976).
[5] P. G. de Gennes, *Scaling Concepts in Polymer Physics* (Cornell University Press, Ithaca, 1979).
[6] J. des Cloizeaux and G. Jannink, *Polymers in Solution: Their Modelling and Structure* (Clarendon, Oxford, 1990).
[7] M. Daoud, in *Fractals in Science,* edited by A. Bunde and S. Havlin (Springer-Verlag, Heidelberg, 1994), p. 163.
[8] R. Everaers, I. S. Graham, and M. J. Zuckermann (unpublished).
[9] S. Redner, J. Phys. A **13**, 3525 (1980).
[10] K. Kremer and K. Binder, Comput. Phys. Rep. **7**, 259 (1988).
[11] C. Domb, J. Chem. Phys. **38**, 2957 (1963).
[12] N. Eizenberg and J. Klafter, J. Chem. Phys. **99**, 6088 (1993).
[13] Z. V. Djordjevic, I. Majid, H. E. Stanley, and R. J. dos Santos, J. Phys. A **16**, L519 (1983).
[14] S. Havlin and D. Ben-Avraham, Adv. Phys. **36**, 695 (1987).
[15] J. P. Bouchaud and A. Georges, Phys Rep. **195**, 127 (1990).
[16] A. Bunde, S. Havlin, and H. E. Roman, Phys. Rev. A **42**, 6 (1990).
[17] A. Bunde, and S. Havlin, *Fractals and Disordered Systems* (Springer-Verlag, Heidelberg, 1991).
[18] J. Klafter, G. Zumofen, and A. Blumen, J. Phys. A **24**, 4835 (1991).
[19] H. E. Roman and P. Alemany, J. Phys. A **27**, 3407 (1994).
[20] A. Bunde and J. Dräger, Physica A **202**, 371 (1994); Philos. Mag. B **71**, 721 (1995); Phys. Rev. E **52**, 53 (1995).
[21] F. T. Wall, S. Windwer, and P. J. Gans, Math. Comput. Phys. **1**, 217 (1963).
[22] H. J. Herrmann and H. E. Stanley, J. Phys. A **21**, L829 (1988).
[23] U. A. Neumann and S. Havlin, J. Stat. Phys. **52**, 203 (1988).
[24] H. E. Roman, Phys. Rev. E **51**, 5422 (1995).